ISSN 1063-7761, Journal of Experimental and Theoretical Physics, 2021, Vol. 133, No. 4, pp. 455–460. © Pleiades Publishing, Inc., 2021.
Russian Text © The Author(s), 2021, published in Zhurnal Eksperimental'noi i Teoreticheskoi Fiziki, 2021, Vol. 160, No. 4, pp. 527–533.

SOLIDS AND LIQUIDS

Self-Diffusion in Liquid and Solid Alloys of the Ti–Al System: Molecular Dynamics Simulation

G. M. Poletaev

Polzunov Altai State Technical University, Barnaul, 656038 Russia

e-mails: gmpoletaev@mail.ru

Received May 4, 2021; revised May 4, 2021; accepted May 14, 2021

Abstract—Self-diffusion in liquid and solid alloys of the Ti–Al system, including pure Ti and Al metals, is investigated using the molecular dynamics method. Apart from intermetallides Ti_3Al, TiAl, and $TiAl_3$, disordered alloys with analogous ratios of the components are considered. For these systems, self-diffusion characteristics are obtained separately for Ti and Al atoms. According to obtained results, the diffusion activation energy of both liquid and solid alloys of the Ti–Al system considerably depends on the concentration of components, repeating approximately the phase diagram. The activation energy of disordered alloys turns out to be smaller by 1.5 times than that for ordered alloys. No appreciable difference in the diffusion mobilities of atoms of different species is detected in analysis of self-diffusion in melts and in solid disordered alloys. However, in the case of ordered alloys (especially intermetallides Ti_3Al and TiAl), this difference is manifested clearly: Al atoms diffuse much more slowly than Ti atoms. Diffusion in intermetallide $TiAl_3$ is anisotropic: main displacements of atoms occur along atomic planes with alternating Ti and Al atoms in the $D0_{22}$ superstructure packing.

DOI: 10.1134/S1063776121090041

1. INTRODUCTION

Intermetallic compounds of the Ti–Al system and alloys on their basis have a high potential for applications, in particular, in aerospace and motor-car industries, as high-temperature structural materials owing to the combination of such their properties as low density, high yield stress at high temperatures, and high resistance to oxidation and corrosion [1–5]. The main technological process for obtaining intermetallides and alloys is based on diffusion that is a complex and multifactorial process in such systems. The diffusion zone at the boundary between Ti and Al can contain simultaneously solid ordered and disordered phases as well as liquid mixtures with different concentrations of components [6–9]. Diffusion characteristics such as diffusion activation energy differ significantly not only in these phases, but also depend on the concentration of components in a simple mixture [8–11]. The knowledge of the diffusion characteristics and mechanisms separately in different phases of the Ti–Al systems is required for deeper understanding of the processes occurring during high-temperature synthesis; such information is also very important for the entire field of investigation and obtaining of Ti–Al alloys.

By now, experimental data on self-diffusion of Al and Ti atoms have been accumulated predominantly for TiAl and Ti_3Al intermetallides [11–13]. Self-diffusion in disordered alloys, in the $TiAl_3$ intermetallide, and in corresponding melts has not been studied comprehensively because of their strong tendency to ordering. The studies of melts encounter a number of difficulties in such investigations: high temperature and chemical reactivity, crystallization at container walls, and the lack of appropriate isotopes in the case of Al [14–16].

An alternative conceptual approach to creating databases of transport and thermodynamic properties of alloys can be based on simulation by the molecular dynamics method. Such an approach is completely free of limitations imposed in experimental investigations. In contrast to experiment, molecular dynamics simulation makes it possible to directly analyze the composition and temperature dependences of the relations between various transport and thermodynamic properties of alloys.

This study is aimed at obtaining the self-diffusion characteristics for liquid and solid alloys of the Ti–Al system using the molecular dynamics method. Ordered and disordered alloys with compositions $Ti_{75}Al_{25}$, $Ti_{50}Al_{50}$, and $Ti_{25}Al_{75}$, as well as pure Ti and Al metals, are considered.

2. DESCRIPTION OF THE MODEL

Interatomic interactions in the Ti–Al system are described using the potentials of the embedded atom model (EAM) from [17], where these potentials have

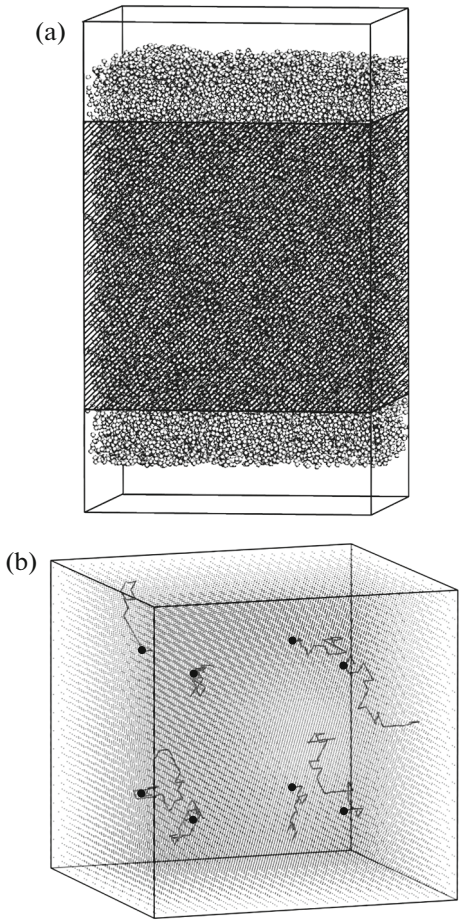

Fig. 1. Models for investigating self-diffusion: (a) in melt (diffusion was estimated from the displacement of atoms in the dark region); (b) in crystal (bullets show the initial positions of eight vacancies and examples of displacement of atoms as a result of self-diffusion).

been obtained based on comparison with the results of experiments and ab initio calculations for various properties and structures of Ti and Al metals and intermetallides Ti_3Al and TiAl. These potentials proved to be effective in various investigations and were successfully tested for a wide spectrum of mechanical and structural–energy properties of alloys of the Ti–Al system [17–19].

Calculation cells contained from 30000 to 50000 atoms and had the form of right parallelepipeds (Fig. 1). Over all axes, periodic boundary conditions were used. When diffusion in liquid metals was simulated, free space (at the top and bottom of Fig. 1a) was created additionally for the melt could freely change its volume upon a change in temperature and during initial melting of the original crystal. The melt structure was simulated in the model by specifying the calculation cell temperature higher than the melting point and by maintaining this temperature during the time sufficient for complete melting of the entire cell. The diffusion coefficient in this case was determined from the displacement of atoms only in the dark region in Fig. 1a to exclude the influence of the free surface.

In simulating solid alloys with a certain specified temperature, thermal expansion was taken into account based on the data from [17]. The temperature in the model was specified in terms of the initial velocities of atoms in accordance with the Maxwell–Boltzmann distribution. To maintain temperature at a constant level during the simulation, the Nose–Hoover thermostat [20, 21] was used.

Diffusion in crystals in the thermodynamic equilibrium conditions is known to follow predominantly the vacancion mechanism. Naturally, there exist comparatively more "mobile" defects (e.g., interstitial atoms and bivacancies). However, their equilibrium concentrations are much lower than the concentration of vacancies, and their contribution is very small against the background of the vacancion mechanism [22]. The vacancion diffusion activation energy is the sum of the vacancy formation energy E_v^f and activation energy E_v^m of vacancy migration. In the molecular dynamics method, both these energies are determined separately as a rule. For determining the migration energy, two methods are used, which can be referred to as the static and the kinematic methods [22]. If the trajectory of migration of a defect is known, the energy barrier on the migration path is determined by the static method. This method is characterized by a higher accuracy, but has two drawbacks: the impossibility to obtain another important diffusion characteristic—preexponential factor D_0 in the corresponding Arrhenius equation, and also the necessity to analyze and take into account the individual contributions from all possible variants of migration of the given defect (especially in multicomponent systems with a low-symmetry structure).

The other (kinematic) method is less accurate than the static method, but makes it possible to determine the effective values of the migration energy and the preexponential factor. It involves the determination of the temperature dependence $D'(T)$ of the diffusion coefficient when the preset number of defects of the given type have been introduced into the calculation cell. The probability of a diffusion act in the simulated crystal volume in this case is substantially higher than in the thermodynamic equilibrium conditions. For recalculating the diffusion coefficient in equilibrium conditions, the data of vacancy formation energy are used.

In this study, the kinematic method is used for determining diffusion characteristics. In analysis of diffusion in solid metals and alloys, eight vacancies were initially introduced into calculation cells with account for the stoichiometric relation between the components (Fig. 1b). When diffusion was simulated in the liquid phase, there was no need in introducing

additional defects. In this case, the recalculation of the diffusion coefficients for the equilibrium concentration as in the case of solid alloys was not required either.

The self-diffusion coefficient was calculated using the Einstein relation

$$D = \frac{\langle \Delta r^2 \rangle}{6t}, \quad (1)$$

where $\langle \Delta r^2 \rangle$ is the mean square displacement of atoms relative to their initial positions and t is the time. The molecular dynamics experiments for determining the diffusion coefficient lasted from 0.5 to 2 ns. The integration time step in the molecular dynamics method was 2 fs.

3. SELF-DIFFUSION IN LIQUID MIXTURES OF THE Ti–Al SYSTEM

Figure 2 shows the dependences of ln D on $10^3/T$, which were obtained in the model for Ti–Al mixtures, as well as for pure metals Ti and Al. All diffusion coefficients had values in the range 10^{-8}–10^{-9} m^2/s. For the temperatures considered here, these values are in good agreement with the experimental results and data by obtained other researchers [14, 16, 23–27]. All these dependences are strictly linear, indicating that the same diffusion mechanism with the same activation energy operates in the given temperature interval.

In accordance with the Arrhenius equation, the self-diffusion activation energy can be determined from the angular coefficient of the linear dependence,

$$Q = -k\frac{d(\ln D)}{d(T^{-1})} = -k\tan\alpha, \quad (2)$$

where k is the Boltzmann constant. The preexponential factor is calculated from the intersection of the line with the ordinate axis:

$$\ln D(0) = \ln D_0. \quad (3)$$

The resulting values of Q and D_0 are given in Table 1. The diffusion activation energy in liquid Al and Ti almost coincides with the real experimental data [25–27] (given in italics in Table 1), which speaks in favor of authenticity of the interatomic interaction potentials used here. As expected, the activation energy in alloys considerably depends on the concentration of the components. This dependence is nonmonotonic and, beginning from 0.28 eV for pure Al and ending at 0.57 eV for pure Ti, has a peak at 0.72 eV for the identical ratios of the components. It should be noted that in the liquid phase, a predominance of a certain component has not been detected for any of the mixture compositions—the diffusion characteristics for Ti and Al prove to be close in the same conditions. This effect was noted in [14], where self-diffusion in liquid mixtures of the Ni–Al system was studied by the molecular dynamics method; however, for a higher concentration of one of the mixture component, the diffusion coefficient for this element prevailed. Such a difference in the results is probably due to a higher binding energy for Ni–Al as compared to that for the Ti–Al system.

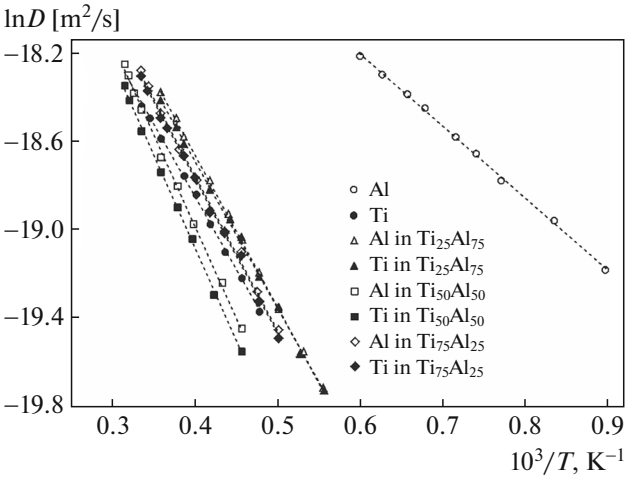

Fig. 2. Dependences of ln D on $10^3/T$ for liquid Ti–Al mixtures and pure metals Ti and Al.

4. SELF-DIFFUSION IN SOLID ALLOYS OF THE Ti–Al SYSTEM

As mentioned above, the self-diffusion in solid metals and alloys of the Ti–Al system was simulated by introducing eight vacancies into the initial calculation cell. The temperature dependences of self-diffusion coefficient D' (corresponding to the given concentration of vacancies) strictly obeyed the Arrhenius law like in the case of melts. Figure 3 shows the dependences of ln D' on $10^3/T$ for ordered and disordered

Table 1. Characteristics of self-diffusion for liquid alloys of the Ti–Al system

Diffusing element	Q, eV	D_0, m^2/s
Al in Al	0.28	0.88×10^{-7}
	0.274 [25]	*1.79 × 10^{-7}* [25]
	0.280 [26]	
Ti in Ti	0.57	0.89×10^{-7}
	0.563 [27]	*1.14 × 10^{-7}* [27]
Al in $Ti_{75}Al_{25}$	0.60	1.17×10^{-7}
Ti in $Ti_{75}Al_{25}$	0.60	1.15×10^{-7}
Al in $Ti_{50}Al_{50}$	0.72	1.54×10^{-7}
Ti in $Ti_{50}Al_{50}$	0.72	1.47×10^{-7}
Al in $Ti_{25}Al_{75}$	0.59	1.21×10^{-7}
Ti in $Ti_{25}Al_{75}$	0.57	1.08×10^{-7}

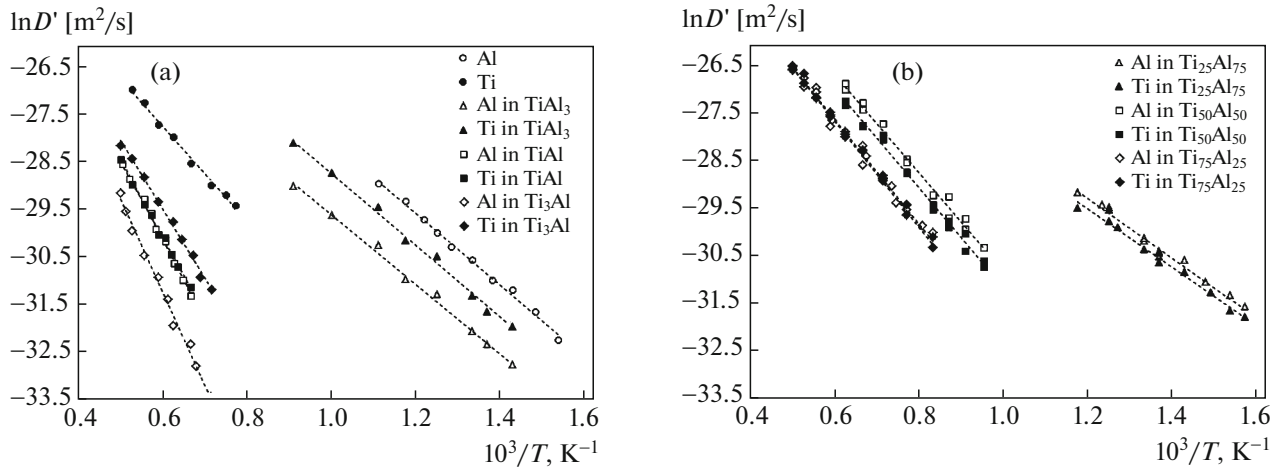

Fig. 3. Dependences of ln D' on $10^3/T$ for (a) ordered and (b) disordered alloys of the Ti–Al system, as well as for (a) pure metals Ti and Al.

alloys with compositions $Ti_{75}Al_{25}$, $Ti_{50}Al_{50}$, and $Ti_{25}Al_{75}$, as well as for pure metals Ti and Al. We considered intermetallides Ti_3Al (superstructure $D0_{19}$), TiAl (superstructure $L1_0$), and $TiAl_3$ (superstructure $D0_{22}$). For studying diffusion in disordered alloys, three calculation cells with different random distributions of Ti and Al atoms were created for each ratio of the components. For obtaining disordered alloys, we used the same type of the crystal lattice as for the ordered alloy with the same ratio of the components, but with additional relaxation of the structure for removing stresses caused by a random distribution of atoms of different species.

For the self-diffusion coefficient in the thermodynamic equilibrium conditions, we can write

$$D = \frac{c_v}{c_v'} D' = \frac{N}{n} D_0' \exp\left(\frac{\Delta S_v^f}{k}\right) \times \exp\left(-\frac{E_v^f + E_v^m}{kT}\right) = D_0 \exp\left(-\frac{Q}{kT}\right). \quad (4)$$

Here, c_v and c_v' are the equilibrium concentration of vacancies at temperature T and that specified in the model, respectively; N is the number of atoms in the calculation cell; D_0' is the preexponential factor obtained after the introduction of n vacancies into the calculation cell; ΔS_v^f is the vacancy formation entropy; and E_v^f and E_v^m are the energies of formation and migration of vacancies, respectively. The right-hand side of expression (4) is the classical Arrhenius law.

Consequently, the preexponential factor in equilibrium conditions has form

$$D_0 = \frac{N}{n} D_0' \exp\left(\frac{\Delta S_v^f}{k}\right). \quad (5)$$

The vibrational component of vacancy formation entropy was determined using the technique described in [22]. For all materials considered here, it was in the interval from $0.3k$ to $0.4k$.

The vacancy formation energies in a two-component ordered alloy upon the removal of A and B atoms are usually different; however, for calculating the diffusion activation energy, it is expedient to use the effective vacancy formation energy in the alloy:

$$\overline{E_v^f} = -kT \ln\left[\frac{N_A}{N}\exp\left(-\frac{E_{vA}^f}{kT}\right) + \frac{N_B}{N}\exp\left(-\frac{E_{vB}^f}{kT}\right)\right]. \quad (6)$$

Here, we have used the assumption that the entropies of formation vacancies A and B are identical. Then we can write the following expressions for the diffusion activations energies of atoms of the A and B components:

$$Q_A = \overline{E_v^f} + \overline{E_{vA}^m}, \quad Q_B = \overline{E_v^f} + \overline{E_{vB}^m}. \quad (7)$$

The effective activation energy of a jump of an atom of species A or B to the vacancy site was determined using formula (2) analogously to the method described in Section 3.

The resulting values of $\overline{E_v^f}$, $\overline{E_v^m}$, Q, and D_0 are given in Table 2, which also contains the data from other works, which were obtained both experimentally [11–13, 17, 28, 29] and by calculating based on the ab initio method [30, 31]. For effective energy of vacancy formation, Table 2 contains values for temperature $0.7T_m$, where T_m is the melting temperature.

Analyzing the data given in Table 2, we note above all a considerable (almost by 1.5 times) difference in the self-diffusion activation energies in ordered and

Table 2. Characteristics of self-diffusion for solid alloys of the Ti–Al system

Diffusing element	$\overline{E_v^f}$, eV	$\overline{E_v^m}$, eV	Q, eV	D_0, m^2/s
Al in Al	0.71	0.65	1.36	7.2×10^{-6}
	0.68 [28, 29]		*1.33* [17]	
			1.47 [11]	*1.71×10^{-4}* [11]
Ti in Ti	1.83	0.85	2.68	2.0×10^{-5}
	1.55 [17]		*3.14* [11]	1.35×10^{-3} [12]
			2.02 [30]	
Al in Ti_3Al ($D0_{19}$)	2.13	1.68	3.81	2.0×10^{-5}
	1.35 [11]		*4.08* [12]	*2.32×10^{-1}* [12]
Ti in Ti_3Al ($D0_{19}$)	*2.24* [31]	1.25	3.38	5.4×10^{-6}
			2.99 [12]	*2.24×10^{-5}* [12]
Al in $Ti_{75}Al_{25}$ (disorder)	1.31	0.96	2.27	4.5×10^{-6}
Ti in $Ti_{75}Al_{25}$ (disorder)		0.95	2.26	4.4×10^{-6}
Al in TiAl ($L1_0$)	2.02	1.46	3.48	1.6×10^{-5}
	1.22 [11]		*3.71* [13]	*2.11×10^{-2}* [13]
Ti in TiAl ($L1_0$)	*1.80* [31]	1.36	3.38	7.9×10^{-6}
			2.59 [13]	*1.43×10^{-6}* [13]
Al in $Ti_{50}Al_{50}$ (disorder)	1.18	0.89	2.07	9.4×10^{-6}
Ti in $Ti_{50}Al_{50}$ (disorder)		0.90	2.08	9.4×10^{-6}
Al in $TiAl_3$ ($D0_{22}$)	1.53	0.63	2.16	1.4×10^{-6}
Ti in $TiAl_3$($D0_{22}$)	*1.46* [31]	0.65	2.18	4.0×10^{-6}
Al in $Ti_{25}Al_{75}$ (disorder)	0.99	0.54	1.53	2.4×10^{-6}
Ti in $Ti_{25}Al_{75}$ (disorder)		0.53	1.52	1.7×10^{-6}

disordered alloys. For this reason, self-diffusion in disordered alloys occurred much more rapidly than in ordered ones. In disordered alloys, like in melts, no significant difference in the diffusion mobilities of atoms of different species was detected. However, this difference was clearly manifested in intermetallides Ti_3Al and TiAl: in this case, Al atoms diffused much more slowly than Ti atom, which is in good agreement with experimental data from [12, 13].

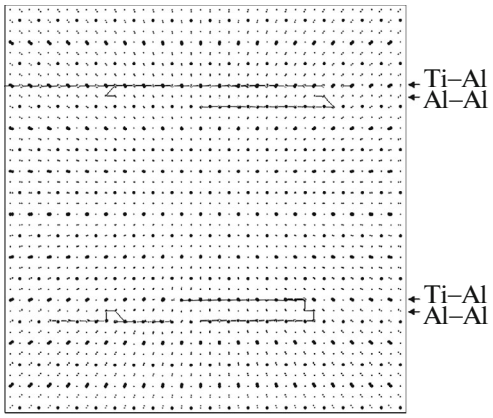

Fig. 4. Diffusion anisotropy in intermetallide $TiAl_3$ with superstructure $D0_{22}$.

It was found in analysis of self-diffusion in intermetallide $TiAl_3$ that is clearly anisotropic by nature: main displacements of atoms occurred in atomic planes with alternating Ti and Al atoms with superstructure $D0_{22}$ (Fig. 4).

5. CONCLUSIONS

Using the molecular dynamics method, we have investigated self-diffusion in liquid and solid alloys in the Ti–Al system, as well as in pure metals Ti and Al. Apart from intermetallides Ti_3Al, TiAl, and $TiAl_3$, we considered disordered alloys with an analogous ratio of the components. For these systems, we have obtained the characteristics of self-diffusion (activation energy and preexponential factor in the corresponding Arrhenius equation) for Ti and Al atoms separately.

According to our results, the diffusion activation energy both in liquid and in solid alloys of the Ti–Al system substantially depends on the concentration of components, approximately repeating the phase diagram. The self-diffusion activation energy for disordered alloys proved to be 1.5 times lower than for ordered alloys.

Analysis of self-diffusion in melts and in solid disordered alloys has not revealed a noticeable difference between the diffusion mobilities of atoms of different species. However, in the case of ordered alloys (especially intermetallides Ti_3Al and TiAl), this difference was manifested clearly: Al atoms diffused much more slowly than Ti atoms. In intermetallide $TiAl_3$, diffusion is anisotropic: atomic displacements mainly occurred in atomic planes with alternating Ti and Al atoms with superstructure packing $D0_{22}$.

FUNDING

This study was supported by the Ministry of Science and Higher Education of the Russian Federation (project no. FZMM-2020-0002).

REFERENCES

1. Y.-W. Kim, J. Metals **46**, 30 (1994).
2. F. Appel, P. A. Beaven, and R. Wagner, Acta Metall. Mater. **41**, 1721 (1993).
3. J. Lapin, in *Proceedings of the Conference Metal-2009, Hradec nad Moravicí*, Česká Republika, May 19–21, 2009.
4. T. Tetsui, Rare Met. **30**, 294 (2011).
5. T. Voisin, J.-P. Monchoux, and A. Couret, in *Spark Plasma Sintering of Materials*, Ed. by P. Cavaliere (Springer, Cham, 2019), p. 713.
6. Q. Wu, J. Wang, Y. Gu, Y. Guo, G. Xu, and Y. Cui, J. Phase Equilib. Diffus. **39**, 724 (2018).
7. N. Thiyaneshwaran, K. Sivaprasad, and B. Ravisankar, Sci. Rep. **8**, 16797 (2018).
8. H. Wu, Sh. Zhang, H. Hu, J. Li, J. Wu, Q. Li, and Zh. Wang, Intermetallics **110**, 106483 (2019).
9. J.-G. Luo, Welding J. 79, 239-s (2000).
10. J. Rusing and Ch. Herzig, Scr. Metall. Mater. **33**, 561 (1995).
11. Y. Mishin and Ch. Herzig, Acta Mater. **48**, 589 (2000).
12. J. Rusing and C. Herzig, Intermetallics **4**, 647 (1996).
13. C. Herzig, T. Przeorski, and Y. Mishin, Intermetallics **7**, 389 (1998).
14. E. V. Levchenko, T. Ahmed, and A. V. Evteev, Acta Mater. **136**, 74 (2017).
15. E. Sondermann, F. Kargl, and A. Meyer, Phys. Rev. B **93**, 184201 (2016).
16. N. Jakse and A. Pasturel, Sci. Rep. **3**, 3135 (2013).
17. R. R. Zope and Y. Mishin, Phys. Rev. B **68**, 024102 (2003).
18. Y.-K. Kim, H.-K. Kim, W.-S. Jung, and B.-J. Lee, Comput. Mater. Sci. **119**, 1 (2016).
19. Q.-X. Pei, M. H. Jhon, S. S. Quek, and Z. Wu, Comput. Mater. Sci. **188**, 110239 (2021).
20. G. M. Poletaev and I. V. Zorya, J. Exp. Theor. Phys. **131**, 432 (2020).
21. G. M. Poletaev and R. Yu. Rakitin, Phys. Solid State **63**, 682 (2021).
22. G. M. Poletaev and M. D. Starostenkov, Phys. Solid State **52**, 1146 (2010).
23. A. Mao, J. Zhang, Sh. Yao, et al., Results Phys. **16**, 102998 (2020).
24. J. Qin, X. Li, J. Wang, and Sh. Pan, AIP Adv. **9**, 035328 (2019).
25. F. Demmel, D. Szubrin, W.-C. Pilgrim, and C. Morkel, Phys. Rev. B **84**, 014307 (2011).
26. F. Kargl, H. Weis, T. Unruh, and A. Meyer, J. Phys.: Conf. Ser. **340**, 012077 (2012).
27. J. Horbach, R. E. Rozas, T. Unruh, and A. Meyer, Phys. Rev. B **80**, 212203 (2009).
28. H. Wollenberger, in *Physical Metallurgy*, Ed. R. Cahn and P. Haasen (Elsevier, Amsterdam, 1983).
29. A. N. Orlov and Yu. V. Trushin, *Point Defect Energies in Metals* (Energoatomizdat, Moscow, 1983) [in Russian].
30. J. R. Fernandez, A. Monti, and R. Pasianot, J. Nucl. Mater. **229**, 1 (1995).
31. A. V. Bakulin and S. E. Kulkova, J. Exp. Theor. Phys. **127**, 1046 (2018).

Translated by N. Wadhwa